This project was carried out by a student from École Polytechnique Fédérale de Lausanne, member of the EPFL Spacecraft Team whose first space mission named CHESS is supported by the EPFL Space Center.

Programming and optimization of algorithms to enable autonomous tracking of satellites with an X-band antenna

Abstract

To communicate with its CHESS satellite, the EPFL Spacecraft Team is developing its own ground station, notably around an X-band antenna, mounted on an X-Y antenna pointing mechanism. Because of the high frequency, it is notoriously harder to follow LEO satellites with an X-band antenna than with standard UHF or even S-band antennas, more commonly used in student satellite projects. The goal of this project is to develop the algorithms to allow the autonomous tracking of satellites by the ground station. The project first investigated the accuracy required by the antenna and available from the satellite TLEs (Two-Line Elements). Then, different algorithms have been devised and tested in simulation to improve the tracking accuracy, via methods of spiral search and gain map modelization. Finally, a calibration procedure for the installation of the antenna has been realized to ensure a correct tracking with minimal corrections required during a satellite pass.

Author:
Aurélien Genin

Supervisor:
Pr. Jean-Paul Kneib

Januray 10, 2025

eSpace
EPFL Space
Center

Contents

1 Introduction

The EPFL Spacecraft Team (EST) is a student team, supervised by eSpace, the EPFL Space Center, which is developing its first space mission named CHESS, standing for Constellation of High-performance Exospheric Science Satellites. Its goal is to fly two 3U CubeSats in orbit around the Earth - one in a low-earth circular orbit, the other one in an elliptical orbit - to study the composition of the exosphere and ionosphere. This mission is developed in collaboration with the universities of Bern and Zurich, which develop the scientific instruments, whereas EPFL develops the satellite platform and the ground station.

As for any satellite mission, it is necessary to communicate with the spacecraft, to receive telemetry and know its health, to send telecommands to the satellite, and to receive scientific measurements made on-board. Depending on the data rate required for these different actions, different frequencies can be used. The common radio frequencies used for space applications are presented in Fig.1.1.

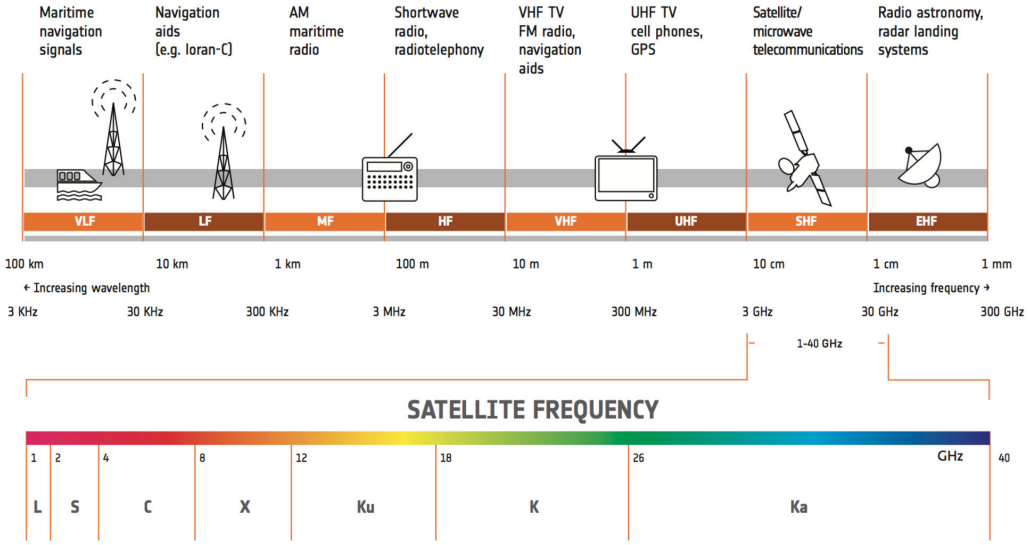

Figure 1.1: *Radio frequency spectrum with examples of applications for the different ranges. Satellites typically used frequency bands from the VHF (300-3000MHz) to the Ka-band (26-40GHz). The higher the frequency, the higher the data rate that can be achieved. Figure from ESA, under ESA Standard License.*

For the CHESS mission, it has been decided to use two frequencies:

- UHF (Ultra High Frequency) for the uplink and downlink of telecommands and telemetry. This frequency is commonly used for student satellite projects, as it is easy to track. The EST already has its own UHF ground station, connected to the SatNOGS network[1].
- X-band for the downlink of scientific data. This frequency is much higher than UHF, and is used for high data rate applications. However, it is much harder to track a satellite with an X-band antenna, as the beamwidth is much smaller than for UHF antennas. The EST is developing its own X-band ground station, with an X-band antenna mounted on an X-Y antenna pointing mechanism.

[1]SatNOGS is an open-source network of ground stations, usually by amateurs or students, that can be used to communicate with satellites and assess their health state

However, to communicate with satellites, it is necessary to know where they are in the sky, and to point the antenna towards them. This tracking needs to be done autonomously, as the satellites passes for Low Earth Orbit (LEO) satellites are short (∼10min) and the ground station will not always be crewed. Moreover, the tracking needs to be accurate, as the beamwidth of the X-band antenna is small (see 1.1), and signal quality will deteriorate if the antenna is not pointing correctly.

1.1 EST X-band antenna

For its ground station, the EST is developing an X-band antenna that will be used for the scientific downlink of the CHESS mission [11]. This antenna uses a 2.4m diameter meshed dish, which will be mounted on an X-Y antenna pointing mechanism. It is expected to be installed on the roof of the ELB building, on the EPFL campus, in the first semester of 2025.

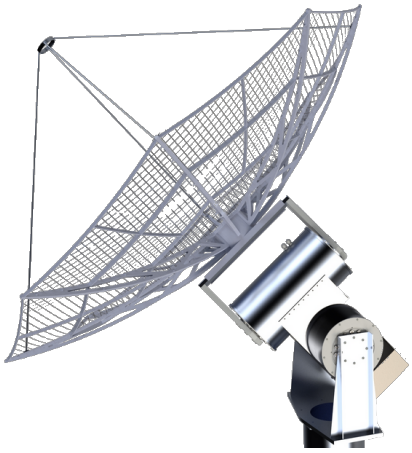

Figure 1.2: *Rendering of the EST X-band antenna, with the 1.5m diameter meshed dish mounted on the X-Y antenna pointing mechanism. Figure from [11].*

Thanks to its large diameter, the antenna achieves a high gain of more than 40dB, which allows for a high data rate communication with the satellite. However, because of the high frequency of the X-band (8-12GHz), the beamwidth of the antenna is small, as can be seen on the antenna radiation profile in Fig.A.1. This beamwidth is generally measured by the Half Power Beam Width (HPBW), which is the angle between the two points on the main lobe of the radiation pattern where the power is half of the maximum (loss of 3dB). For the EST X-band antenna, the HPBW has been simulated to be around 1.1°, which means that the antenna needs to be pointed towards the satellite with an accuracy of less than 0.5° to ensure a good signal quality [8].

1.2 Project objectives

Because of this high accuracy requirement for the tracking of the satellite, some thinking is needed on how to point the antenna precisely towards the satellite. This is less the case with UHF antennas, which have a much larger beamwidth, and can be pointed in the general direction of the satellite without losing too much signal quality. The goal of this project is to develop the algorithms that will allow the autonomous tracking of satellites by the ground station. The project has been divided into several parts:

1. Study of the accuracy required by the antenna and available from the satellite TLEs (Two-Line Elements);
2. Development of different tracking algorithms, based on open-loop and closed-loop tracking, to improve the tracking accuracy;
3. Simulation of the tracking algorithms, to assess their performance and robustness;
4. Development of a calibration procedure for the installation of the antenna, to ensure a correct tracking with minimal corrections required during a satellite pass.

This report presents the work done on these different parts, and the results obtained. Section 2 presents the simulation of satellite passes developed for this project, allowing to compute the link budget with different tracking solutions. Section 3 presents the different tracking algorithms developed, and the results obtained in simulation. Section 4 details the calibration procedure for the installation of the antenna that has been developed to ensure a correct tracking of the satellite with minimal corrections required.

2 Satellite pass simulation

To develop and test different tracking algorithms, it was necessary to simulate passes of a satellite over the ground station. I developed one on Python that can give the position in the sky of the satellite during the pass, and simulate the antenna radiation profile to compute the signal power received by the ground station depending on its pointing. This section presents the different parts of the simulation, from the satellite pass prediction to the link budget computation.

2.1 Satellite pass prediction

To simulate the satellite pass, it is necessary to know the orbit of a satellite. In my simulation, it is possible to define an orbit manually, with the classical Keplerian parameters:

- Semi-major axis a (in km);
- Eccentricity e;
- Inclination i (in degrees);
- Right Ascension of the Ascending Node Ω (in degrees);
- Argument of Perigee ω (in degrees);
- Mean Anomaly M (in degrees).

For real satellites, these parameters are measured in particular by the United States Space Force and published on the Internet on the SpaceTrack and Celestrack websites. They are given in a standard format named Two-Line Element (TLE).

```
ISS (ZARYA)
1 25544U 98067A   08264.51782528 -.00002182  00000-0 -11606-4 0  2927
2 25544  51.6416 247.4627 0006703 130.5360 325.0288 15.72125391563537
```

Figure 2.1: *Example of a TLE for the International Space Station. The different elements describe the orbit of the satellite in Keplerian coordinates, as well as information on the date of the TLE and some data on the satellite.*

TLEs can be used to predict the position of a satellite in the future. For this, the most common algorithm is the SGP4 model. It is a simplified model that can take different forces and perturbations into account. The minimal one is of course the gravitational force of the central body (in our case, the Earth). Perturbations can be added to make the prediction more accurate, such as the atmospheric drag, the gravitational forces of the Moon and the Sun, the oblateness of the Earth... The SPG4 model is implemented in the `poliastro` Python package I used for my simulation [10].

Because of these perturbations, and the uncertainty in the initial orbit measurement, the TLEs and the predicted satellite positions are not perfect. This point has been studied in more details in 3.1.1.

When the orbit of the satellite is known, it is possible to predict the position of the satellite in the sky at any time. This is necessary when doing ground communication with satellites, or for astronomy observations (such as optical satellite surveillance). For this purpose, I developed the `satastro`[2] Python package which enables notably to make the necessary reference frame change to get the position of the satellite in the sky from its cartesian position around the Earth given by SGP4. The position in the sky is given in the Altitude-Azimuth (AltAz) coordinate system, which is the most common one used

[2]Published on GitHub and on PyPi

for ground observations and communication with satellites. The Altitude[3] is the angle between the satellite and the horizon, and the Azimuth is the angle between the satellite and the North direction. This package makes heavy use of the `astropy` package, because the task performed are really close to ones for astronomy [3].

2.2 Link budget simulation

With the `satastro` package, it is possible to compute the position of a, real or simulated, satellite in the sky. For radio communication, it is interesting to also know the signal power received by the ground station, to assess the quality of the link. This is done by computing the link budget, which is obtained by summing the different gains and losses in the communication link between the satellite and the ground.

In my simulation, I computed the link budget for the X-band antenna of the EST ground station. The link budget is given by the following formula:

$$P_{RX} = P_{TX} - L_{FS} + G_{RX} - P_{noise} \tag{2.1}$$

where:

- P_{RX} is the power received by the ground station (in dBW);
- P_{TX} is the power transmitted by the satellite (in dBW);
- L_{FS} is the free space path loss (in dB);
- G_{RX} is the gain of the receiving antenna (in dB);
- P_{noise} is the noise power of the receiving antenna (in dBW).

The noise power is given by the antenna noise temperature, and is computed by Eq.2.2. It represents the total noise of the antenna, i.e. the power when the signal of the satellite is not present.

$$P_{noise} = 10 \log_{10} (k_B T B) \tag{2.2}$$

where:

- k_B is the Boltzmann constant (1.381×10^{-23} J/K);
- T is the noise temperature of the receiver (in K);
- B is the bandwidth of the signal (in Hz);

The free space path loss (FSPL) is simply the loss of power caused by the spread of the signal in space, governed by the inverse square law. It is given by Eq.2.3. The evolution of the FSPL with distance and elevation is given in Fig.A.2.

$$L_{FS} = 20 \log_{10} \left(\frac{4\pi df}{c} \right) \tag{2.3}$$

where:

- d is the distance between the satellite and the ground station (in m);
- f is the frequency of the signal (in Hz);
- c is the speed of light ($299,799,458$ m/s).

The values for the different parameters of the link budget are given in Table 2.1.

[3] To not confuse the reader with the height of the satellite on its orbit, the term elevation is also used for the angular altitude.

Parameter	Value	Reference
P_{TX}	13.2 dBW	CHESS documentation [5]
d	550 to 1800 km	`satastro` simulation
f	10.5 GHz	CHESS documentation [5]
G_{RX}	-30 to 42 dBW	Antenna radiation profile [11]
T	242 K	CHESS documentation [5]
B	10.5Mbps	CHESS documentation [5]

Table 2.1: *Values of the different parameters of the link budget computation.*

The gain of the receiving antenna is obtained from the radiation profile of the EST X-band antenna [11]. It is interpolated to compute the gain of the ground antenna if it doesn't point exactly towards the satellite. The angular separation between the real AltAz position of the satellite in the sky, given by the `satastro` pass simulation, and the commanded AltAz position of the antenna is used to get the actual value for G_{RX} with the radiation profile (see Fig.A.1).

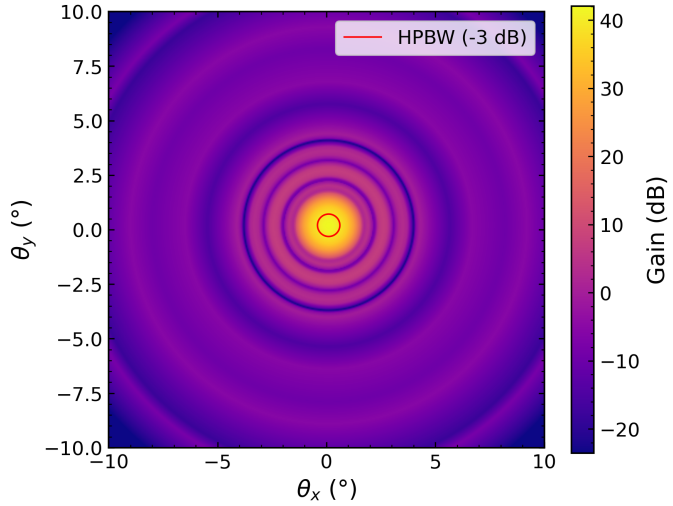

Figure 2.2: *Interpolated radiation profile in 2D. The initial radiation profile comes from [11]. The θ_x and θ_y show offsets (e.g. from the antenna pointing towards the satellite) from the antenna axis.*

To make this link budget simulation more realistic, I added two sources of perturbations:

- Ground antenna pointing uncertainties. Because of mechanical reasons (backlash, weight flexures, vibrations...) and external perturbations (wind), the antenna will not stay perfectly still. I simulated this by adding a random noise (2D Gaussian with a null mean and a modifiable variance) to the antenna pointing, before computing G_{RX}. This adds a noise to G_{RX} with a random distribution that is representative of this pointing inaccuracy.
- Random Gaussian noise to the final P_{RX}. To account for the noise in the measurement of P_{RX}, I added a random Gaussian noise to the simulation, with a null mean and a modifiable variance.

This simulation code enables to look at a complete satellite pass and calculate the received signal power from the ground antenna depending on its pointing in the sky. To visualize this, we can show this power in all the sky, as if the antenna was able to measure the signal power instantaneously in all directions. This is depicted in Fig.2.3 for different moments of the pass. We observe the radiation profile of the receiving antenna from Fig.2.2. The changes in the maximum received power (and of the "background" signal, far from the satellite) show the effect of the free space path loss.

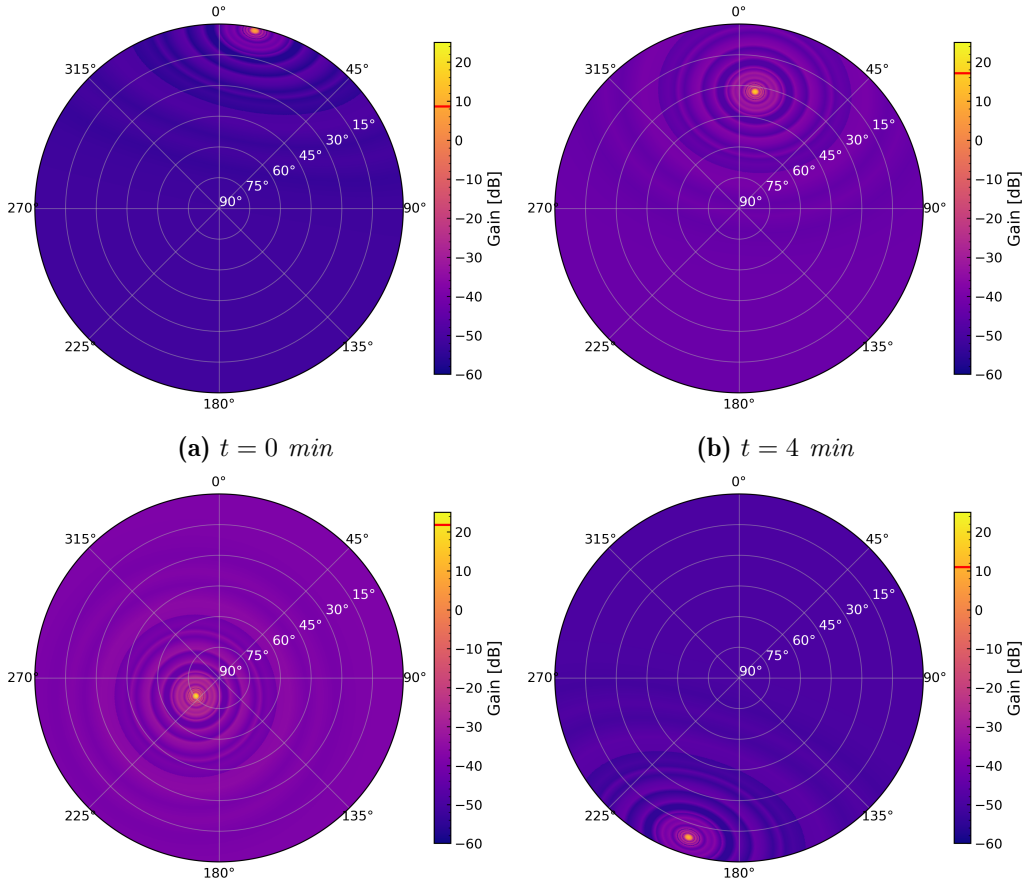

(a) $t = 0$ *min* **(b)** $t = 4$ *min*

(c) $t = 6$ *min* **(d)** $t = 10$ *min*

Figure 2.3: *Simulation of the CHESS satellite passing over the EST X-band antenna. The figures show different moments of the pass and represent the signal power over the full sky. The red line in the colourbar shows the maximum power, i.e. the power if the antenna were pointing perfectly at the satellite.*

3 Tracking algorithms

To communicate with a satellite, it is necessary to point the ground antenna towards the satellite. This pointing requires more or less accuracy depending on the width of the radiation profile of the antenna, and so the frequency of communication. Generally, the higher the frequency is, the more precise the pointing must be. For low frequencies such as HF or VHF, static antennas can even be used since they can easily be made omnidirectional (sensitive to signal in any incoming direction).

In the case of the EST X-band antenna, the radiation profile gives a HPBW of around 1.1°. This therefore requires a pointing accuracy of less than 0.5° to ensure a good signal quality (power loss smaller than 3dB).

The pointing of the satellite with the ground antenna can be performed in different ways. In this project, I investigated four main strategies, that are presented in further details in this section. These strategies differ mainly on the level of feedback they use. They are therefore represented on Fig.3.1 on a spectrum ranging from open-loop to closed-loop. In this figure, open-loop means that the pointing control algorithm uses no information from the antenna receiving signal. On the contrary, closed-loop means that the pointing algorithm uses constantly the measured signal quality to correct itself. An additional strategy, "Calibration" is present on the spectrum. It is different than the others because it is not directly a control algorithm, and is therefore presented in the next section 4.

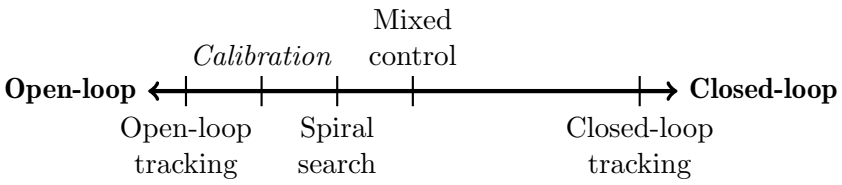

Figure 3.1: *Feedback spectrum of the control algorithms devised to track satellites with a ground antenna.*

3.1 Open-loop tracking

The first strategy is the open-loop tracking. It is the simplest one, as it doesn't require any feedback from the antenna. The pointing of the antenna is computed from the TLE of the satellite, and the antenna is commanded to point towards the predicted position of the satellite. This strategy is the most common one for ground stations, as it is easy to implement and doesn't require any feedback from the antenna. However, it is also the less accurate one, as it doesn't consider the real position of the satellite in the sky, and the real signal quality received by the antenna. In the following sub-sections, we look into the precision that can be achieved with such a tracking strategy.

3.1.1 TLE precision

When tracking a satellite in open-loop, there are two main sources of pointing errors:

- Pointing errors from the antenna. These errors come between the commanded pointing[4] and the real antenna pointing. This error can be caused by a lot of factors: bad calibration, bad referencing with the ground (addressed in 4), mechanical backlash, vibrations, flexures...

[4]Here, and in the rest of this document, pointing is the AltAz coordinates of the antenna or target.

- Position[5] errors of the satellite. These errors come between the real position of the satellite and the measured position given by the TLE, and predicted in time. These errors can be caused by the uncertainty in the initial orbit measurement, and the perturbations that are not considered in the SGP4 model.

Here, we focus on the second source of error. The TLEs are mainly published by the United States Space Force, and are available for most of the satellites in orbit. They are used by the SGP4 model to predict the position of the satellite in the sky. However, the TLEs are not perfect, and the predicted position of the satellite can be off by a few km.

The satellite position error is generally given in the UVW local quasi-inertial reference frame.

- U axis is in the direction of the geocentric radius vector (from the centre of the Earth to the satellite);
- V axis complements the base such that $V = W \times U$ (in the direction of the velocity vector of the satellite);
- W axis is in the direction of the angular momentum vector of the satellite orbit (perpendicular to the orbit plane).

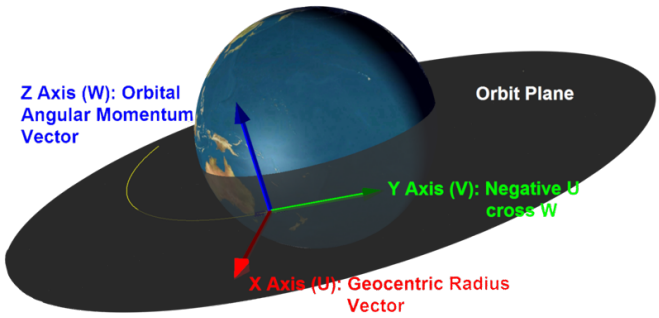

Figure 3.2: *Defintion of the UVW local quasi-inertial reference frame. Adapted from ai-solutions.com.*

The UVW reference frame also appears in the literature as the RTN (Radial-Transverse-Normal) or LVLH (Local Horizontal-Local Vertical) frames. Their axis are perfectly aligned, but in different orientation.

Different studies investigated the precision of the TLEs for LEO satellites [2, 6, 9]. They measured their uncertainty at the time of measurement, and the evolution of this uncertainty over time. The results of these studies are presented in Table 3.1. The uncertainty is the error in position at the time of measurement of the TLE. The drift is the evolution of the satellite position from the TLE over time.

Parameter	**Uncertainty** (km)	**Drift** (km/day)	**Uncertainty evolution** (km/day)
U	0.1	0.02	0.1
V	0.5	3	0.5
W	0.15	∼0	0.15

Table 3.1: *Errors and drifts in the UVW reference frame of the TLEs.*

Commonly, it is considered that the TLEs are precise to ±1 km when measured, and lose 1-2 km/day in precision [9]. This means that the satellite position can be off by 1-2 km

[5]Here, and in the rest of the document, position is the cartesian position of the target in space.

from the predicted position at the time of the pass. This error is not negligible as 1 km at 500 km of altitude is already 0.1° of pointing error.

3.1.2 Antenna tracking accuracy

Here, we look into the impact of the TLE error on the tracking accuracy of the antenna. We consider that the antenna is perfectly pointing towards the satellite (an hypothesis that is relaxed in 4), and that the only source of error is the TLE position error. We compute the maximum error in pointing that can be caused by the TLE error.

For this, we use the `satastro` package to simulate a satellite pass directly over the ground antenna. This trajectory is imagined as being the predicted satellite position from the TLE. The TLE error is implemented by adding a UVW position offset to the satellite position, giving the "real" satellite position. The error is kept constant over the pass, as the pass is short and thus the drift is negligible. The antenna is simulated to point at the predicted satellite position, and the error in pointing is computed by the angular separation between the predicted and real satellite positions. This simulation gives a maximal angular pointing error over a pass, for a given UVW position error. By repeating this process for different position errors, we get a 3D map of the maximal pointing error as a function of the UVW position error. This map is presented in Fig.3.3. It has been realized with 31x31x31 samples, in the $[-10, 10] \times [-8, 8] \times [-8, 8]$ km range UVW space.

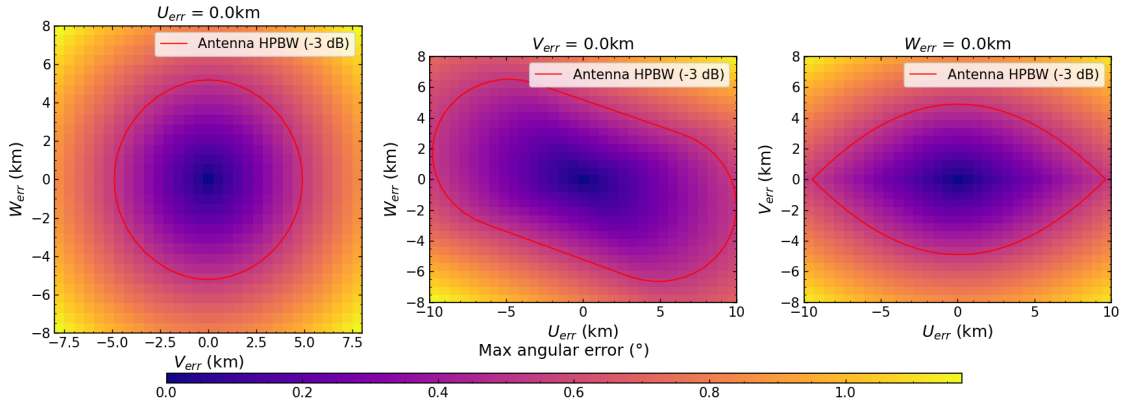

Figure 3.3: *Maximal pointing error of the antenna as a function of the UVW position error of the satellite over a pass. The error is computed by the angular separation between the predicted and simulated satellite positions. The figure shows three slices of the 3D map in the three UVW directions.*

The 3D map shows that the UVW position error has a different impact on the pointing error depending on the direction of the error. The U error has the smallest impact on the pointing error, as the satellite is mis-placed in the "up/down" direction, which is more or less the direction of the vector from the antenna to the satellite[6]. The W and V errors have similar impacts as they are more or less perpendicular to the antenna-satellite vector.

It is interesting to look at how the HPBW of the EST antenna fits into this analysis. The HPBW shows a 3dB loss from the maximum antenna gain. It is around 1.1 for the EST antenna, which means that the antenna can tolerate a pointing error of around 0.5° to ensure a good signal quality. It is shown on Fig.3.3, where we observe that it spans a

[6]This approximation is worse when the satellite appears at a low elevation, but then it is also further than when it's at the zenith, making the pointing error smaller.

relatively large area of the UVW error space. Another way to look at it is to display the HPBW boundary as volume in the 3D UVW space. This is shown in Fig.3.4.

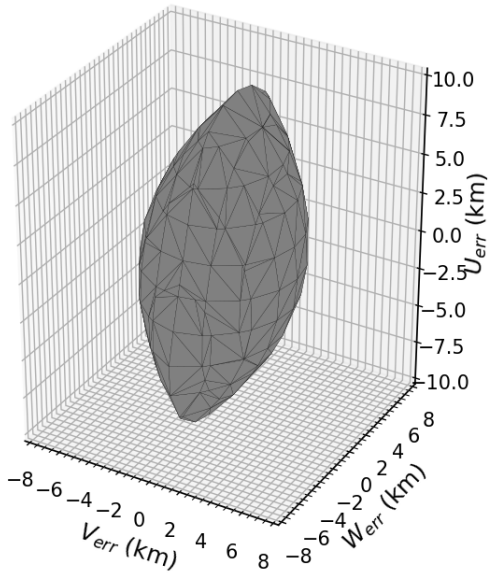

Figure 3.4: *Envelope of the HPBW of the EST antenna (1.1° in diameter) in the UVW space. It represents the satellite position error values that are acceptable so that the satellite still falls in the HPBW of the antenna, losing a maximum of only 3dB of signal quality.*

As previously, we observe that the U coordinate is the less critical, as the HPBW is more or less aligned with this axis. The V and W coordinates are more critical, as the HPBW is perpendicular to these axes. The HPBW volume is a good representation of the acceptable UVW error values for the satellite position, as it shows the values that are acceptable so that the satellite still falls in the HPBW of the antenna, losing a maximum of only 3dB of signal quality.

From this envelope, we can measure that maximal position error tolerable to stay within the HPBW is 4.8 km. By comparing it to the TLE errors and drifts from Table 3.1, we can see that open-loop tracking is precise enough with TLEs that are less than ∼2 days old. This is generally the case for LEO satellites, as the TLEs are updated every ∼24h. This conclusion is however only correct if the antenna is properly calibrated so that it points exactly where it is commanded to point. This point is addressed in 4.

This theoretical analysis is also confirmed by radio-amateurs already following satellites and downlinking data in X-band. It is especially the case of Scott Tilley which tracks satellites in LEO only using the TLEs, as well as some deep space missions, with antennas in his backyard.

3.2 Spiral search

As explained before, tracking errors come from two main sources: errors in the satellite position from the TLE, and errors in the antenna pointing. The previous open-loop strategy is sufficient if the errors in the antenna pointing are small enough. These could be corrected by a calibration procedure, which is presented in 4. However, if the antenna pointing errors are too large, simply tracking the TLEs might not be sufficient for communication. In this case, a dose of signal quality feedback is required. This is the goal of

the spiral search strategy, which is presented in this section.

3.2.1 Principle

The idea of the spiral search strategy is to scan a portion of the sky around the predicted satellite position, to find the best signal quality and correct for the difference in pointing.

This type of strategy is also used in optical astronomy to find a target when the pointing of the telescope is not precise enough. After an initial guess pointing, the telescope scans around this position until the targeted object is found. This search is usually performed with a spiral pattern, which is the most efficient way to cover an area from a starting guess that should be not too far from the target.

In optical astronomy, more advanced techniques use plate solving to navigate to a target. This method is based on the analysis of the images taken by the telescope to find stars and locate them on the celestial sphere. This allows to know exactly where the telescope is pointing in the sky, and how to correct its pointing towards the target.

However, this method is not possible for radio communication because the ground station antenna doesn't measure an image but a simple signal power. The problem faced here is can be expressed as an optimization problem:

$$\text{maximize} \quad f(x) \quad \text{with} \quad x \in \mathbb{R}^2$$

where $f(x)$ is the signal quality received by the antenna (in our case, we use P_{RX} from Eq. 2.1), and x is the antenna pointing, with two coordinates (e.g. AltAz).

The actual problem is more complex because the function f depends on the satellite position and therefore changes over time. In 3.2.2, we focus on this optimization problem with a static point source.

Moreover, the function f is not known and can only be sampled by the antenna at different pointings. The optimization problem must therefore be solved in real time, in the real world, and not in software. Such problems are generally solved with well-known algorithms such as gradient descent or evolutionary algorithms. However, they are not directly suitable for our application. Gradient descents tend to get stuck in local optimals. Fig.2.2 shows that the function f is far from a simple convex function and has a lot of local maxima (the secondary lobes of the antenna). Evolutionary algorithms are more robust to this problem, but they are not suitable for our application because they require a lot of samples to converge to a good solution, meaning the antenna would have to move to a lot of positions, taking too much time. This is not possible in our case because the satellite is moving and the antenna must be constantly corrected.

The solution that has been chosen is to use a spiral search pattern, which is a simple and efficient way to scan an area around a point. It also guarantees to find the maximum as long as the spiral pattern is well chosen[7] and the maximum is within the spiral's radius. The spiral search pattern is shown in Fig.3.5. It is defined as an Archimedean spiral by three parameters: the total radius of the spiral R, the distance between two arms of the spiral r and the distance between two points of the spiral d. The spiral points are calculated by the algorithms presented in B.

3.2.2 Gain map modelization

To find the satellite, we need to maximize the signal-to-noise ratio (SNR). As explained before, this is done by sampling the SNR in different positions around the predicted

[7]The distance between the points of the spiral shall be in the order of the HPBW to not miss it.

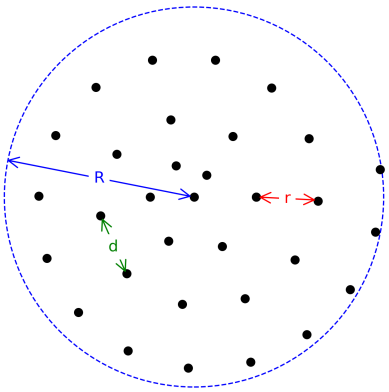

Figure 3.5: *Defintion of the spiral search pattern. The spiral is an Archimedean spiral, except the inner points where it is a logarithmic spiral for better filling of the space.*

satellite position, using a spiral search pattern. A naive way to locate the satellite would be to simply select the point where the SNR is the highest. However, this method would not be very precise as it would entirely depend on the sampling points.

A better solution is to use kriging (also known as Gaussian process regression) to model the function f from the sampled measurements, and then use an optimization algorithm to find the maximum of the model. This method has the big advantage of being precise even with a relatively low number of samples.

Each sample represents a measurement of the SNR at a given antenna pointing. However, measuring the SNR is not a simple task with an antenna. It requires to integrate the measured signal power over a certain time window to have an accurate measure of the signal and of the surrounding noise. Through different searches, a time window of 1s seems reasonable for our case. The total time of the spiral search is therefore very dependent on the number of points.

For the kriging, we used the OpenTurns package developed by researchers and engineers at Airbus, EDF, IMACS, ONERA ,and Phimeca. [4]. It is tested with a simulated point source and the radiation profile of the EST X-band antenna. The gain map is therefore the one given in Fig.2.2.

Kriging predicts the value of a function by computing a weighted average of the sampled values around it. The weights are computed using a covariance function. They define the correlation between the function values at different points. The choice of this covariance function impacts the smoothness of the resulting modelled function. Kriging also provides an uncertainty at every points, based on this covariance, which can be used to select the best following points to sample (see 3.3). For the modelization of the gain map, we used the Matern 1/2 covariance function, a standard kernel that worked well in our case.

Once the gain map has been modelled using kriging, we use a simple evolutionary algorithm to find the maximum of the modelled function. We used the `GN_ESCH` algorithm from NLopt, implemented in OpenTurns.

Fig.3.6 shows the result of the kriging modelization of the gain map, as well as the predicted position of the source compared to the real one. The spiral used in this example has R=5°, r=2° and d=2°, composed of 24 points. For additional realism, the SNR measurements are noisy (±1 dB and ±0.1 ° on the pointing). The distance between the satellite and the predicted position is 0.52°.

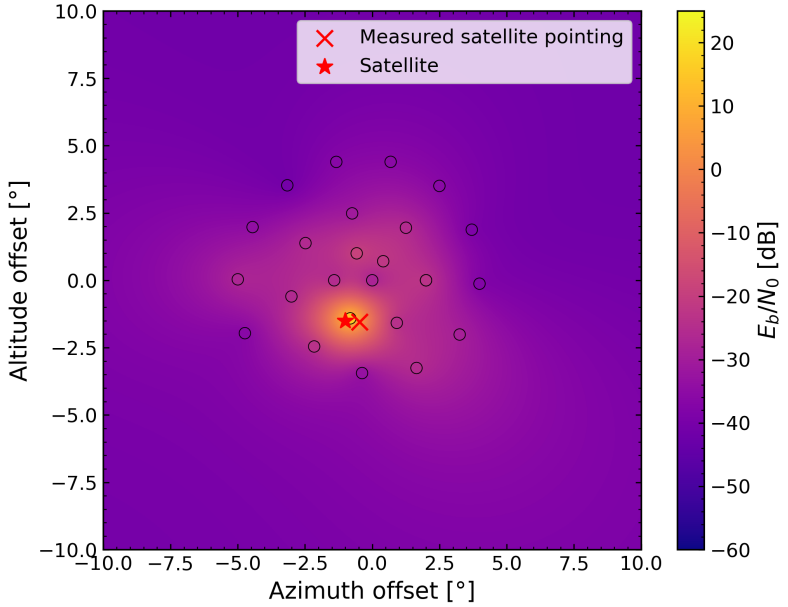

Figure 3.6: *Modelization of the gain map using kriging. The satellite is simulated as a fixed point source, offset from the center. The black circles show the sampled points using a spiral search with R=5° r=2° and d=2°. The distance between the satellite and the predicted position is 0.52°.*

The resulting map doesn't show the intricate details present in Fig.2.2, because of the low number of samples, and of the noise. However, it still finds a maximum that is very close to the real position of the satellite, within the HPBW of the antenna. The following parts explain how this modelization with spiral search can be used to correct the tracking of the satellite during a pass.

3.2.3 Antenna pointing correction

The spiral search and gain map modelization gives a measurement of the angular offset between the real satellite pointing and the commanded antenna pointing, at the time of measurement. This value can be used for two purposes:

- To correct the antenna pointing error. The offset is used to correct the commanded pointing of the antenna, so that it points towards the real satellite position. This is done by adding the offset to the commanded pointing.
- To estimate the TLE error on the position of the satellite. The offset is used to correct the predicted position of the satellite, so that the tracking is more precise (in particular at the highest elevation of the pass) and future passes over the ground station are more accurate. This strategy is studied in 3.2.4.

The simplest use is to correct the antenna pointing offset. This can be used if the calibration of the antenna is not good enough to point within 0.5° (half the HPBW) of the satellite. The correction is done by adding the offset to the commanded pointing of the antenna.

This offset can be measured very early on the pass, as soon as the satellite is in view of the ground segment. This means that it can be performed at low elevation (below 20°), before the downlink starts. Therefore, no communication time would be lost by performing this correction. It is however necessary that the satellite transmits a continuous X-band beacon during that time so that the antenna can locate it.

The angular offset is not necessarily constant during the pass, for two main reasons:

- The measured angular offset at low elevation integrates the TLE position error. Therefore, the correction is not purely the antenna pointing error, but also the TLE error. However, the effect of the TLE error is on the satellite position and not directly on the pointing. The conversion from satellite position error to angular pointing error is not constant over the pass, as the satellite moves in the sky (it is more important at high elevation). This effect is observed and studied in 3.4.
- If the antenna tracking speed doesn't match exactly the satellite angular speed, then the pointing offset will change over time. To counteract this loss in calibration, the antenna mount motors will have to be controlled in closed-loop to ensure precise tracking of the commanded speed.

This strategy is very efficient to correct the antenna pointing error if the calibration is not sufficient. It uses a simple open-loop tracking of the TLE, with a correction at the beginning of a pass to take the antenna pointing offset into account. Because it can be done at low elevation, the impact on communication time is minimized.

3.2.4 TLE error correction

A second objective of the spiral search strategy is to measure and correct the error of the TLE on the satellite position. This is done by finding the UVW position error which gives the angular pointing offset measured by the spiral search and kriging at the time of measurement. This search is done using standard optimization algorithms, along with the `satastro` package to calculate the satellite corrected position and pointing.

However, this problem is complex because many different solutions exist. The angular pointing offset describe a line from the ground station towards the real satellite position. Multiple UVW errors can bring the satellite to this line as shown on Fig.3.7. To avoid non-sense results, the UVW error is constrained to nearby positions, using the standard positions errors and drifts from Table 3.1.

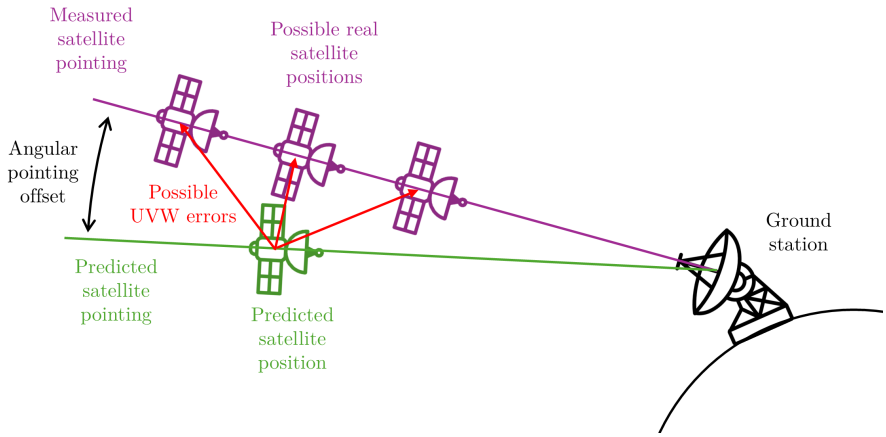

Figure 3.7: *Concept of the UVW error estimation from the angular offset measurement. It shows how multiple solutions of the UVW error exist with this simple method.*

As explained previously, the UVW position error has a large impact on the pointing at high elevation only. Therefore, trying to estimate the position error using a spiral search at low elevation is almost impossible because the uncertainty in the angular pointing offset is larger than the effect of the position error.

To measure this, simulations have been made with the `satastro` package. Multiple UVW errors have been tested in a Monte-Carlo strategy: a gaussian distribution has

been associated to the three UVW error coordinates based on the values from Table 3.1, and UVW error samples were drawn from these distributions. Then, the spiral search has been simulated at different elevation of the satellite pass. With the angular pointing offset measured, the UVW error has been estimated and compared to the real one used for the simulation. Finally, the pass is simulated again by tracking a virtual satellite whose position is calculated using the estimated UVW error. This allows to measure the maximum pointing error throughout the pass, after the correction. The results are presented in Fig.3.8.

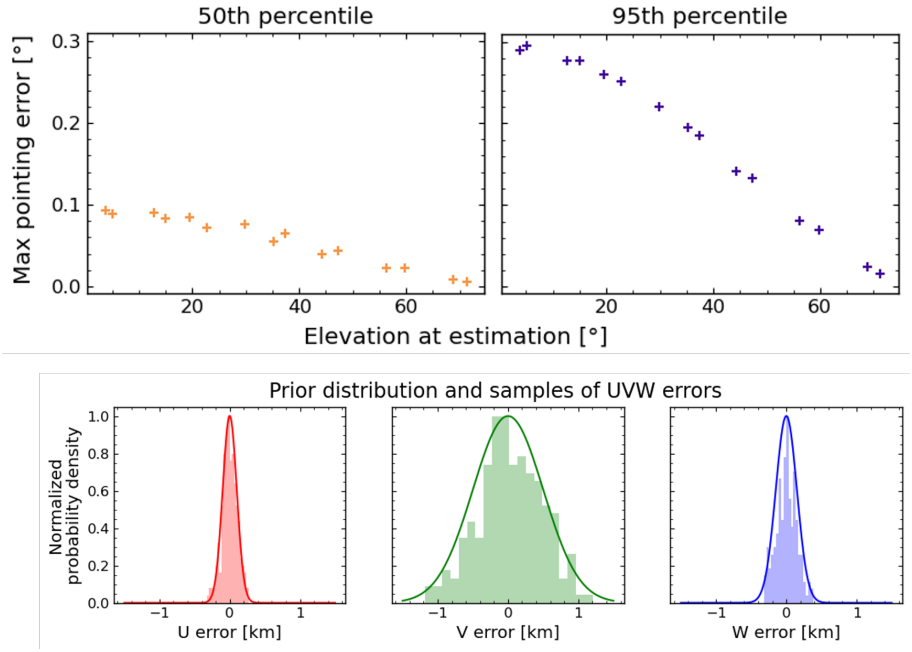

Figure 3.8: *Statistical analysis of the UVW error estimation and correction. The figure shows the 50th and 95th percentile of the maximum pointing error throughout the pass, after a UVW position error correction. An example of read of this figure is: When the TLE error estimation is performed when the satellite is at 40° elevation, the resulting pointing error during the pass after the correction is smaller than 0.15° for 95% of the UVW errors. The bottom plots show the prior distributions used for the simulated UVW errors, according to the values from Table 3.1.*

The statistical study shows that the UVW error estimation is very precise only at high elevations. As expected, when performed at low elevation, the resulting pointing error after the correction is the same as tracking the TLE with no corrections at all on the satellite position. Performing the UVW error estimation at an elevation higher than 40° halves the pointing error throughout the pass. However, when the satellite is that high in the sky is also the time when it is downlinking data. Therefore, it is not possible to perform large antenna motions because the signal quality would be lost, and the communication would be compromised. This is the trade-off between robustness and communication that is studied in 3.3.

A solution to this issue is to use a mixed control strategy, combining a large spiral search at low elevation to correct for the antenna calibration, and a small spiral search (smaller than HPBW) at high elevation to correct for the position error and measure a more precise TLE. This strategy is presented in 3.4.

3.3 Closed-loop tracking

The spiral search strategy is a first-step towards a closed-loop control. However, it is still mostly open-loop because it only uses feedback from the signal quality very loosely to correct the tracking at the start of a pass. A closed-loop control would use the signal quality feedback constantly to correct the antenna pointing and ensure it stays locked on the satellite.

3.3.1 Principle

The idea of the closed-loop tracking is to constantly monitor the SNR received by the antenna, and to constantly correct the antenna pointing to maximize it. This is however a very hard task, for different reasons.

As explained in 3.2.1, the SNR measurements are not instantaneous and the control would have to be performed at a low frequency (<1 Hz). Moreover, because of free space path losses, and noise, the maximum SNR constantly changes during the pass. It is not possible to give a target value for the SNR, and the closed-loop control will have to constantly look for the maximum.

This introduces the problem of knowing that the antenna is tracking the maximum and not some local maximum (side lobes) or a value that was maximal at the start of the pass but is no longer later. The question for the control is therefore the following: How to be sure that the maximum has been found? The only solution for that is to voluntarily sample locations that are not the maximum. This is however problematic because these samples would render the communication impossible. This trade-off between communication and tracking robustness is the focus of this study of the closed-loop strategy.

The control strategy is based on kriging, as with the spiral search presented in 3.2.2. As explained there, kriging produces a model of the gain map (the distribution of SNR in the sky) from a few sampled positions. Moreover, it gives the uncertainty of the model at every point. This value shows how confident the model is at a given point. It is small at the sampled locations, and larger the further from them we go. The idea of Bayesian optimization is to update this model with new samples to efficiently locate the maximum of the function. It is useful when evaluating the function is expensive and should therefore be done a minimal number of times. It is the case here because one SNR measurement takes time. This is done by selecting the next samples using two criteria:

- Exploring regions with high uncertainty to make sure the maximum is not hidden there;
- Exploiting regions with high predicted value to find the maximum.

Multiple algorithms exist to perform Bayesian optimization. The one used in this work is the EfficientGlobalOptimization (EGO) algorithm, implemented in OpenTurns [7]. It is a good compromise between exploration and exploitation, and is efficient in finding the maximum of a function with a low number of samples.

The idea for the closed-loop control is to constantly update the kriging model of the gain map with a fixed temporal memory. Samples that are too old are progressively removed and new samples are selected using EGO. This ensures that the model is always up to date.

To make sure that the communication is good and consistent enough during the pass to downlink data from the satellite, the exploration of EGO must be contained within the HPBW of the antenna. This therefore requires a first spiral search step to come close to the maximum, and then the closed-loop control can be used to lock on it. This idea is developed in 3.4.

3.3.2 Results

Closed-loop control has been tested using the simulation developed for this project. EGO has shown to be not suitable for our application. Because it tries to build a confident model and find the maximum with certainty, it must move to regions of low SNR but high uncertainty to confirm that the maximum is not hidden there. This exploration makes the communication impossible, and costs too much during a pass. The research pattern produced is shown on Fig.3.9.

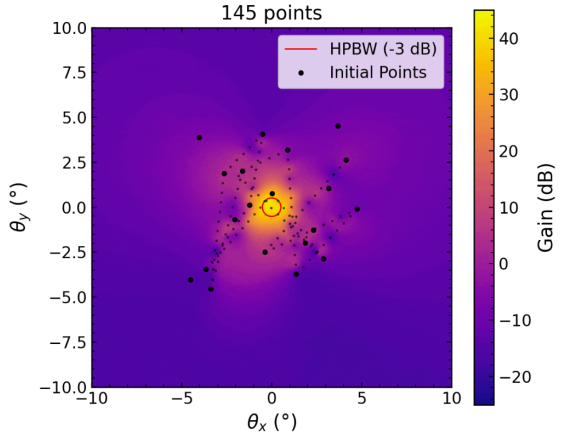

Figure 3.9: *Result of the EGO algorithm for the gain map modelization. It shows exploration over a $\pm 5°$ range around the predicted satellite position, with a large disparity, not suitable for communication.*

To minimize the effect on communication, another strategy has been tested. Instead of using EGO, the next samples are calculated using a very small spiral search contained within the antenna HPBW. The kriging model is still produced and updated with a fixed time horizon, but the exploration is limited. This uses the hypothesis that the antenna is already pointing towards the satellite when the closed-loop control is activated. The centre of this spiral is constantly updated to be the maximum of the kriging model. The result of this strategy is shown in Fig.3.10.

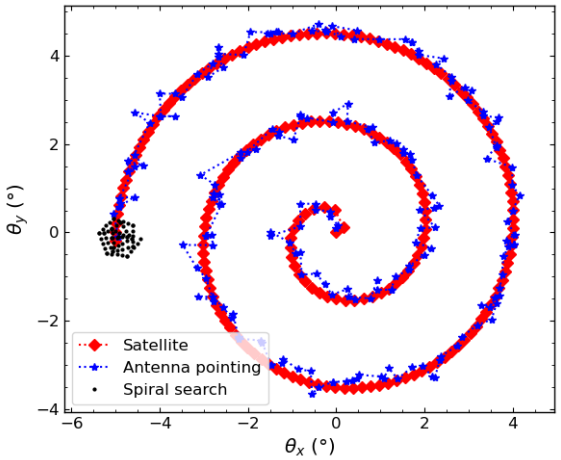

Figure 3.10: *Motion of the antenna in closed-loop spiral control. The antenna (blue) is tracking the satellite that is simulated to move in a large spiral (red). The spiral (black) used for this is contained within the HPBW of the antenna to ensure correct communication.*

Using simulation, it is possible to test this control strategy over a full satellite pass. During this pass, the angular pointing error and the antenna gain (based on the radiation profile) are monitored. This enables a statistical analysis over the whole pass to know the mean and percentiles on the signal quality. These results are presented in Fig.3.11.

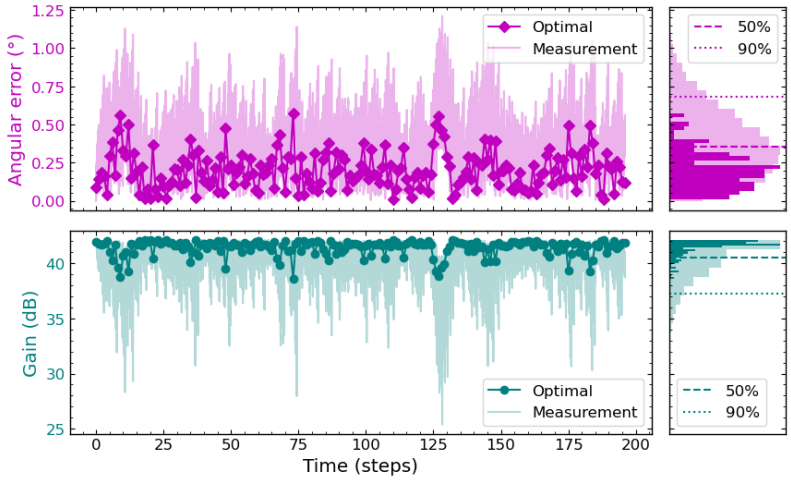

Figure 3.11: *Statistical analysis of the closed-loop control strategy. The figure show the evolution of the angular pointing error and the antenna gain during the tracking of a satellite depicted in Fig.3.10. The bold lines show the optimal value found by the kriging model at every time, whereas the lighter lines show the antenna positions. The plots on the left show the statistical analysis over the full simulation, with the 50th and 95th percentiles.*

It can be observed that although the optimal values found by the kriging model are generally very good, some measurements are far from the satellite and therefore results in large losses in signal quality. This could be reduced by using a smaller spiral, but then the exploration would be too limited and the tracking would be very prone to errors. This is the trade-off between robustness and communication that is further studied in 3.4.

From these results, it can be concluded that the closed-loop control is not suitable for our application. Although closed-loop is generally preferred over open-loop for its robustness, it is not the case here. That is because the measured value, SNR, is also the one that should be maximized for communication, with tight constraints.

Another option for closed-loop control would be to use a separate feed mounted on the antenna. The feeds used for this purpose generally have a very strong null on the feed axis in their radiation profile. The objective of the closed-loop control is therefore to minimze the signal received by this guiding feed. This option has not been further studied in this project because of its cost and complexity added to the ground station.

3.4 Mixed control

The final tracking strategy studied in this project is a mixed control. This strategy uses some elements from previous strategies to combine the robustness of the open-loop tracking with the precision of the closed-loop control. The idea is to use a large spiral search at low elevation to correct the antenna pointing, and smaller spiral searches at higher elevation to correct the TLE error and the rest of the antenna pointing.

This strategy has been tested in simulation using the same tools as before. To make it easier to use, the `radiosat` Python package has been developed[8]. It incorporates the

[8]Published on GitHub and PyPi

computation of the link budget using the ground station antenna radiation profile, as well as the free space path loss and other effects presented in 2.2. It also includes the kriging and spiral searches presented in 3.2.2.

Using this simulation tool, the mixed control strategy has been tested over a full satellite pass. The results are presented in Fig.3.13. They compare the open-loop tracking with an antenna pointing error of (here, 1.1°) and a satellite position error (here, 1.3 km), to the ideal tracking values as well as to the mixed control. The latter uses two spiral searches to correct the antenna tracking of the satellite. The first one is a coarse spiral with a radius of 3° and 17 points, performed at 15° elevation of the satellite. The second one is a finer spiral with a radius of 1° and 12 points, performed at 40° elevation of the satellite. The second spiral can be used to correct a simple antenna pointing offset, or try to estimate the TLE position error. The best results have been observed with a simple antenna pointing offset correction.

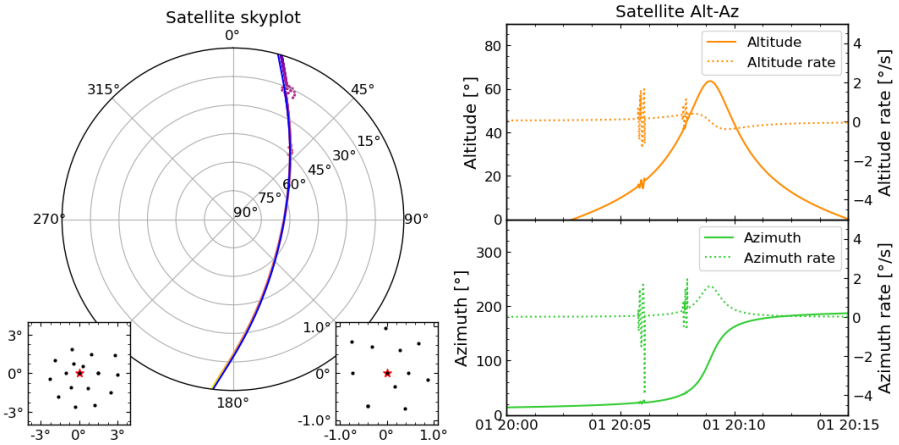

Figure 3.12: *Simulation of mixed control over a full satellite pass. The left figure shows the trajectory of the satellite in the sky (blue) as well as the pointing of the antenna (purple). The smaller plots show the two spiral search patterns used. The plots on the right show the evolution of the altitude and azimuth positions (plain) and rates (dashed) over the tracking.*

Fig.3.13 shows that the pure open-loop strategy is not sufficient to downlink data from the satellite over the pass if the antenna pointing is not well enough calibrated. The corrected open-loop solves this issue using the first large spiral search, reaching only a 2 dB loss to the ideal value. An additional small spiral search at high elevation helps to minimize the effect of the TLE error at the highest elevation of the pass. The mixed control strategy is therefore a good compromise between robustness and precision, and may be the best strategy for tracking a satellite with a ground antenna if the calibration is not sufficient.

3.5 Discussion

During this project, multiple tracking algorithms have been studied and tested in simulation. The open-loop tracking is the simplest and most robust strategy, but it might not be sufficient if the antenna is not well calibrated, an issue assessed in 4. The spiral search strategy is a good way to correct the antenna pointing error, but it is not precise enough to correct the TLE error. The closed-loop control is the most precise strategy, but it is not suitable for our application because of the trade-off between robustness and communication. **The mixed control strategy is a good compromise between the two, and**

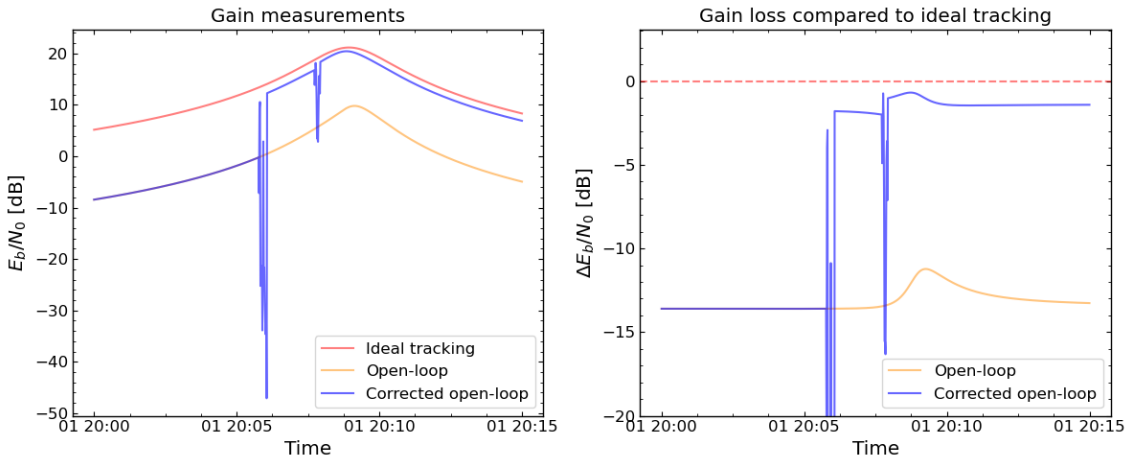

Figure 3.13: *Comparison of the signal power received by the antenna during the pass between open-loop tracking, mixed control (corrected open-loop) and ideal values. The left figure shows the evolution of the signal power over the pass, whereas the right figure shows the difference to the ideal value at any time.*

may be the best strategy for tracking a satellite with a ground antenna.

The diagram presented in Fig.3.14 tries to summarize the links between the different pointing and position measurements and predictions. It was quite complex to navigate between these different parameters, and to find which are available and usable. The diagram also shows thumbnail of some figures present in this report, to better illustrate which interactions and elements they represent.

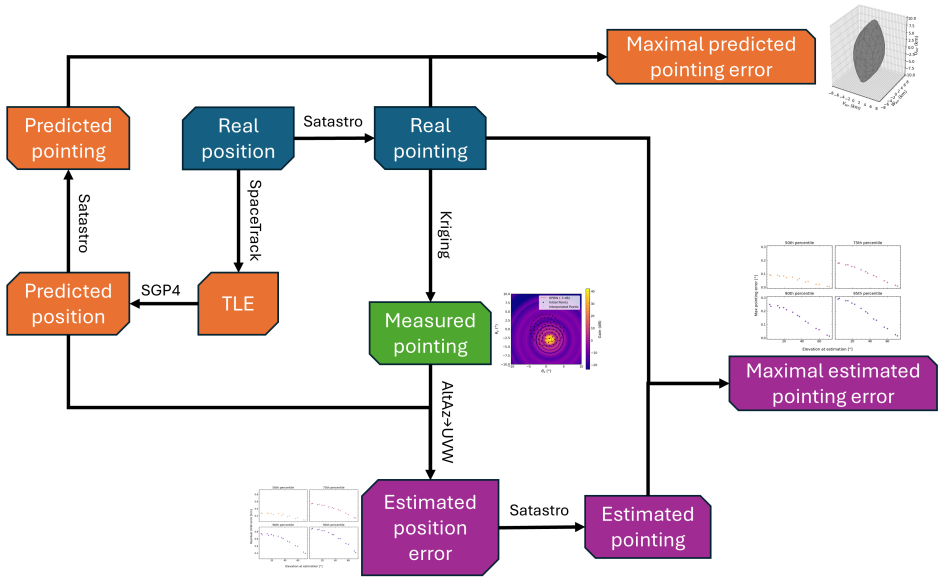

Figure 3.14: *Diagram showing the different control strategies for tracking a satellite with a ground antenna. It depicts the link between the different pointing and position measurements and predictions. The colours separate the parameters based on their origin: real (blue), measured (green), predicted (orange), and estimated (purple).*

4 Antenna installation and calibration

As explained in 3.1, the antenna needs some level of calibration to be able to track the satellite during a pass. The better this calibration is, the easier the tracking will be. In the ideal case, open-loop tracking would be usable directly based on the TLEs, with no need for spiral searches or closed-loop control. In this project, calibration of the antenna represents the relationship between the commanded pointing of the antenna (AltAz position in the sky) and the actual pointing. In this section, we study the impact of installation errors on calibration and how to measure them and correct them or take them into account in the control.

4.1 Antenna control

As can be seen on Fig.1.2, the EST X-band antenna uses an XY mount. In astronomy and ground stations, three main types of mounts exist to move the telescope or antenna and point it towards the sky:

- The alt-azimuth (AltAz) mount, which moves the instrument in altitude (horizon-zenith) and azimuth (north-south). It is the simplest and most common mount, but it presents a "keyhole" effect, where the mount must move very quickly to track an object at high elevation.
- The equatorial mount, which moves the antenna in right ascension (around the Earth's rotation axis) and declination. It is more complex because of the alignment of one axis with the Earth's rotation axis. It is used in astronomy to track celestial objects by turning only one motor and to avoid field rotation.
- The XY mount, which moves the antenna in two orthogonal axes, the first one being horizontal. It is a simple mount broadly use in ground stations because it solves the "keyhole" effect of the AltAz mount to track satellites.

Although the EST antenna uses an XY mount, it is more practical to use the AltAz coordinates to predict and visualize a satellite pass. It is therefore necessary to calculate the rotation angles for the XY mount required to point the antenna towards the targeted AltAz coordinates. This is performed using two rotation matrices ($\mathbf{R_X}$ and $\mathbf{R_Y}$, one per motor) to go from the Earth's ground reference frame to the antenna reference frame.

XY to AltAz (forward problem)

Let's define the Earth's ground reference frame as $(\mathbf{x_0}, \mathbf{y_0}, \mathbf{z_0})$, with $\mathbf{z_0}$ pointing towards the zenith, $\mathbf{x_0}$ pointing towards the north, and $\mathbf{y_0}$ pointing towards the west. The antenna reference frame is defined as $(\hat{\mathbf{x}}, \hat{\mathbf{y}}, \hat{\mathbf{z}})$, with $\hat{\mathbf{z}}$ pointing along the antenna axis, and $\hat{\mathbf{x}} = \mathbf{x_0}$ and $\hat{\mathbf{y}} = \mathbf{y_0}$ when the antenna is pointing towards the zenith. The rotation matrices are defined using axis-angle rotation with the following equation:

$$\mathbf{R_u}(\theta) = \begin{bmatrix} u_x^2\,(1-\cos\theta)+\cos\theta & u_x u_y\,(1-\cos\theta)-u_z\sin\theta & u_x u_z\,(1-\cos\theta)+u_y\sin\theta \\ u_x u_y\,(1-\cos\theta)+u_z\sin\theta & u_y^2\,(1-\cos\theta)+\cos\theta & u_y u_z\,(1-\cos\theta)-u_x\sin\theta \\ u_x u_z\,(1-\cos\theta)-u_y\sin\theta & u_y u_z\,(1-\cos\theta)+u_x\sin\theta & u_z^2\,(1-\cos\theta)+\cos\theta \end{bmatrix}$$

The XY mount is modelled using two rotation matrices $\mathbf{R_X}$ and $\mathbf{R_Y}$, defined by the equations below, where θ_X and θ_Y are the rotation angles of the motors, chosen so that the antenna points towards the zenith when $\theta_X = \theta_Y = 0$.:

$$\mathbf{R_X} = \mathbf{R_{x_0}}(\theta_X) \qquad \mathbf{R_Y} = \mathbf{R_{(R_X y_0)}}(\theta_Y) \tag{4.1}$$

This definition ensures that $\hat{\mathbf{z}} = \mathbf{R_Y R_X z_0}$, correctly modelling the XY mount. The associated AltAz pointing of the antenna are then calculated using the following equations:

$$\begin{bmatrix} \text{Alt} \\ \text{Az} \end{bmatrix} = \begin{bmatrix} \arcsin\left(\hat{\mathbf{z}} \cdot \mathbf{z_0}\right) \\ -\texttt{atan2}\left(\hat{\mathbf{z}} \cdot \mathbf{y_0}, \hat{\mathbf{z}} \cdot \mathbf{x_0}\right) \end{bmatrix} \tag{4.2}$$

where `atan2` is the four-quadrant inverse tangent function from `numpy`.

Using numerical calculations, we can create abacuses to easily visualize the AltAz pointing corresponding to XY motor commands. These abacuses are shown in Fig.4.1.

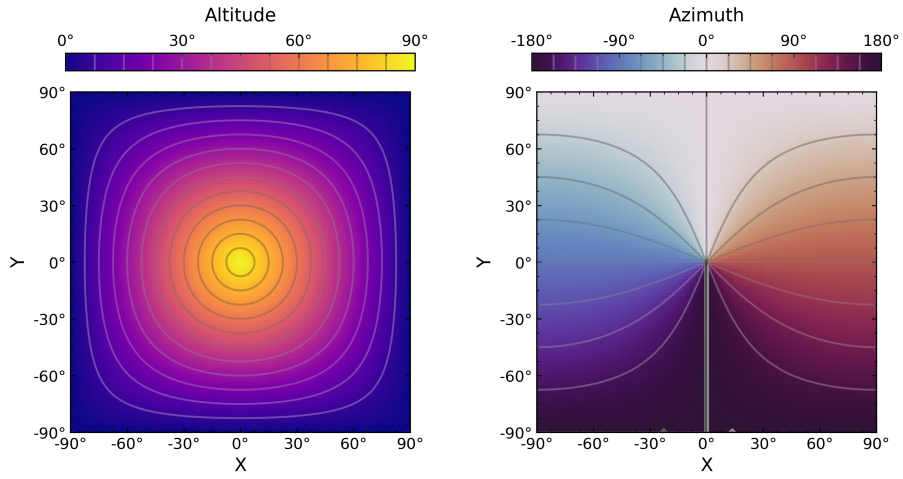

Figure 4.1: *Abacuses showing the AltAz pointing of the antenna corresponding to XY motor commands.*

AltAz to XY (inverse problem)

To command the XY mount, it is necessary to be able to convert AltAz coordinates to XY motor commands. This requires the inverse problem of the previous one. It is non-trivial to solve because the $\mathbf{R_Y}$ matrix is defined using $\mathbf{R_X}$, and because the $\hat{\mathbf{x}}$ and $\hat{\mathbf{y}}$ are vectors are not known from the AltAz coordinates since they don't have a physical meaning. The solution is to use multiple projections to find the correct ones. The first step is creating the $\hat{\mathbf{z}}$ antenna pointing vector.

$$\hat{\mathbf{z}} = \begin{bmatrix} \cos(\text{Alt})\cos(\text{Az}) \\ -\cos(\text{Alt})\sin(\text{Az}) \\ \sin(\text{Alt}) \end{bmatrix} \tag{4.3}$$

Then, it is possible to compute θ_X by projectinf $\hat{\mathbf{z}}$ on the $(\mathbf{y_0}, \mathbf{z_0})$ plane:

$$\hat{\mathbf{z}}^{\mathbf{1}}_{\perp} = \hat{\mathbf{z}} - \left(\hat{\mathbf{z}} \cdot \mathbf{x_0}\right)\mathbf{x_0} \tag{4.4}$$

$$\theta_X = \pm \arccos\left(\frac{\hat{\mathbf{z}}^{\mathbf{1}}_{\perp} \cdot \mathbf{z_0}}{||\hat{\mathbf{z}}^{\mathbf{1}}_{\perp}||}\right) \tag{4.5}$$

We then define $\mathbf{R_X} = \mathbf{R_{x_0}}(\theta_X)$ and use it to calculate θ_Y by projecting $\hat{\mathbf{z}}$ on the $(\mathbf{R_X x_0}, \mathbf{R_X z_0})$ plane:

$$\hat{\mathbf{z}}_{\perp}^{2} = \hat{\mathbf{z}} - (\hat{\mathbf{z}} \cdot \mathbf{R_X y_0})\, \mathbf{R_X y_0} \tag{4.6}$$

$$\theta_Y = \pm \arccos\left(\frac{\hat{\mathbf{z}}_{\perp}^{2} \cdot \mathbf{R_X z_0}}{||\hat{\mathbf{z}}_{\perp}^{2}||}\right) \tag{4.7}$$

The previous equations give four possible combinations of (θ_X, θ_Y). The correct one is chosen by computing the AltAz pointing for each pair using the forward problem and selecting the one that is the closest to the original AltAz coordinates.

Similarly to Fig.4.1, it is possible to create abacuses to visualize the XY motor commands corresponding to AltAz pointing. These abacuses are shown in Fig.4.2.

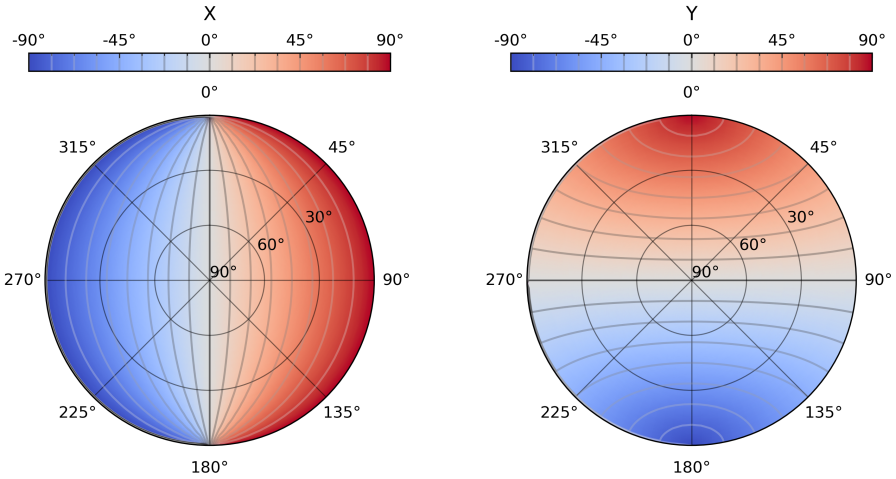

Figure 4.2: *Abacuses showing the XY motor commands required for any AltAz pointing of the antenna.*

4.2 Impact of installation errors

The modelization of the XY mount as presented is based on the hypothesis that the mount's base is installed perfectly with respect to the ground's reference frame. However, in reality, this is not the case, or it should be thought in advance. For our case, there are two sources of installation errors:

- levelling: the mount's base may not be perfectly horizontal (i.e. not orthogonal to the zenith).
- Azimuth alignment: the mount's base may not be perfectly referenced to the north (i.e. the X motor's axis azimuth is not precisely set).

These two errors have a direct impact on the antenna pointing. If they are not considered, the antenna control has no absolute reference of the physical world, and it wouldn't be able to point precisely towards a direction in the sky (let alone a satellite).

To study the effect of these errors, they have been modelled in the simple XY mount model presented in the previous section as three additional rotation matrices. The azimuth alignment is modelled as a rotation around $\mathbf{z_0}$, and the levelling is modelled as two rotations around $\mathbf{y_0}$ and $\mathbf{x_0}$. These matrices are applied before the $\mathbf{R_X}$ and $\mathbf{R_Y}$ matrices in the XY to AltAz conversion. It is then possible to calculate numerically the difference between the pointing with and without these errors. The results are presented in Fig.4.3.

As can be seen in Fig.4.3, each installation error has an impact on a different zone of the sky. The combination of the different sources of errors brings an important error

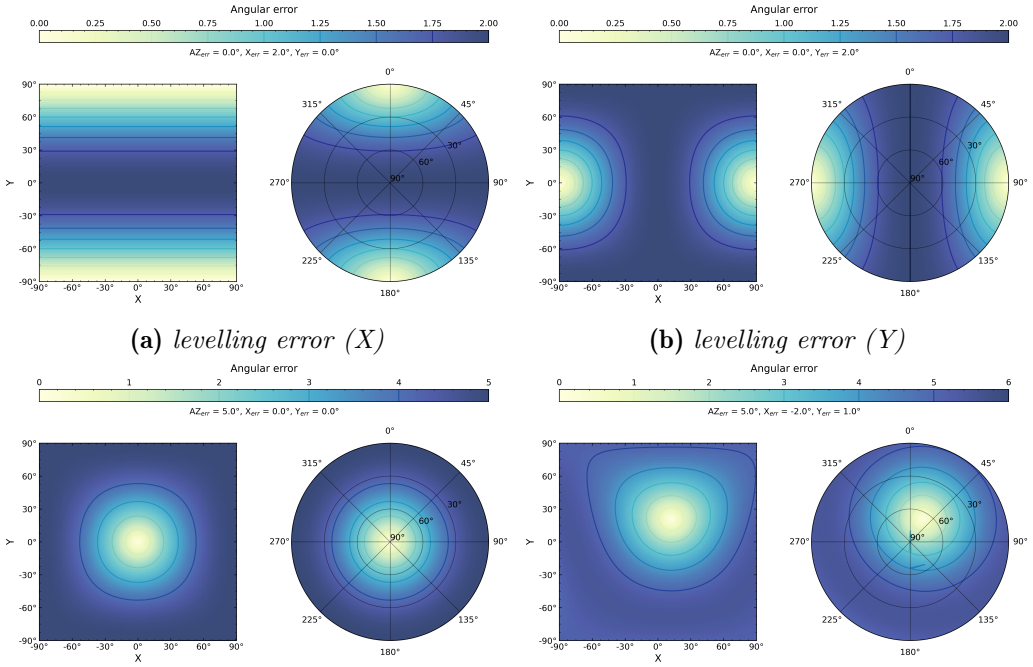

(a) *levelling error (X)*

(b) *levelling error (Y)*

(c) *Azimuth alignment error*

(d) *Composite error*

Figure 4.3: *Effect of the mount installation errors on the antenna pointing. The figures show the difference between the pointing with and without the errors. The different figures show the isolated effect of the three components, and the combination of all of them. In each figure, the left plot is in the X-Y motors plane, and the right plot is in the Alt-Az plane.*

to almost the complete celestial hemisphere. Moreover, the pointing error is not uniform across the sky, meaning that correcting it is more complex than a single constant. To correct this error, the three components of installation errors must be either nullify, or at least measured and considered in the control.

At first order, the maximal pointing error in the sky is the sum of the three components of the installation errors. To use open-loop tracking of a satellite, this maximal pointing error must be smaller than half the HPBW of the antenna (0.55° for the EST X-band antenna). This means that all three errors must be corrected or measured to $\sim 0.15°$.

4.3 Calibration procedure

To calibrate the antenna's mount, it is necessary to measure the installation errors, and then be able to either correct them or take them into account in the control. Taking them into account through software seems easy because it only adds simple rotation matrices to the XY to AltAz conversion problem.

Correcting the errors mechanically are however the solution commonly used for ground stations (or telescopes). This is performed by making sure the base (the piece between the ground and the mount) is perfectly horizontal and referenced to the north. This is done using a level and a compass. To enable corrections, the base is generally designed with screws to adjust the level (three screws to tilt the base plate) and the azimuth (a push-pull screw to rotate the base plate, or simple slots for the three previous screws). This mechanical solution can be observed on Scott Tilley's X-band antenna mount installation. However, in the case of the EST antenna, this solution has been considered too complex. Moreover, the mount has already started production and it would be complicated to adapt

it for this. The base is not yet fully designed, and some possibility for corrections there would be a good idea.

In the case where mechanical corrections are not possible, it would still be doable to measure the installation errors. This can be done using a precise level and compass, placed on the mount's base.

To further verify the mount installation error measurements, and precise them, it is possible to use a geostationary satellite. These satellites are always at the same position in the sky, and therefore can be used as a reference to measure the pointing error of the antenna, without the need for continuous tracking. This is the easiest way to measure the pointing accuracy of the antnna's mount. For this, the antenna would be commanded to point towards a GEO satellite which emits X-band (e.g. ES HAIL 1). From there, a spiral search would be conducted manually (or by a program) to find the maximum signal power, indicating the correct pointing of the satellite. The difference between the commanded pointing and the measured pointing is the pointing error for these AltAz coordinates.

By repeating this procedure in multiple directions, it is possible to create a pointing model and estimate the installation errors. A similar procedure is performed in astronomy with stars. In simulation, and by using a simple optimization algorithm to estimate the installation errors, a minimum of two satellites is necessary, and a third one outside of the GEO arc is preferable. This third satellite could be a MEO satellite or one on a Molniya orbit that has a slow movement in the sky.

Finally, the calibration procedure is summarized on the diagram presented in Fig.4.4. It also shows the calibration of the motors to set their zero position, which has been the subject of a previous study [1]. The diagram presents the choice between selecting an open-loop or a spiral-search mixed control for the tracking of a satellite during a pass.

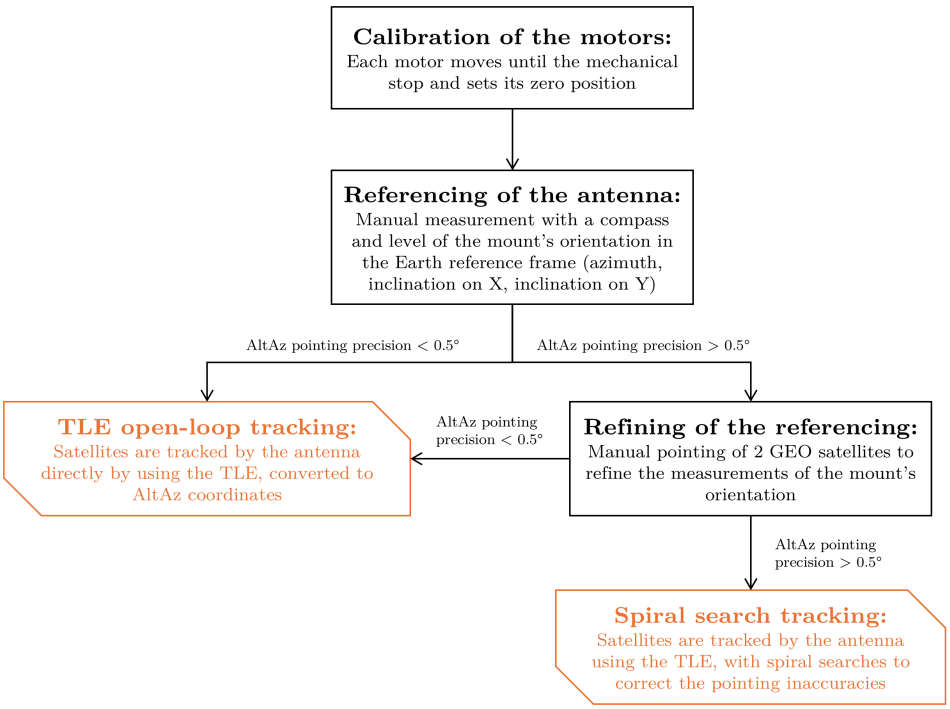

Figure 4.4: *Diagram showing the calibration procedure for the antenna's mount.*

5 Conclusion

This project was about studying how to track a satellite during a pass using the future EST X-band antenna. For this, multiple control strategies have been developed and assessed in a custom simulation. The simulation implemented the orbit and satellite pass computations, as well a standard link budget with an antenna radiation profile. The control strategies studied were open-loop tracking, spiral search, closed-loop control, and a mixed control. The mixed control, using a large spiral at low elevation and a smaller at high elevation, was found to be the best compromise between robustness and precision, and may be the best strategy for tracking a satellite with a ground antenna. However, open-loop tracking would be far simpler and more robust. It requires a correct calibration of the antenna's mount, which we have quantified and proposed a procedure to measure and correct. The next steps of this project will require the physical antenna to be installed, which should arrive in the following semester. From there, the calibration procedure will be performed, and the control strategies will be tested to decide whether open-loop is sufficient or if a mixed control is necessary.

Appendices

A Satellite pass simulation

A.1 Antenna radiation profile

Simulation of the radiation profile of the EST X-band antenna by [11]. It shows the main lobe of the radiation pattern, with a Half Power Beam Width (HPBW) of around 1.1°, as well as side lobes that are much weaker. The structure of the radiation pattern is typical of a parabolic dish antenna, and makes research of the satellite hard because of the small beamwidth and the abundance of local maxima.

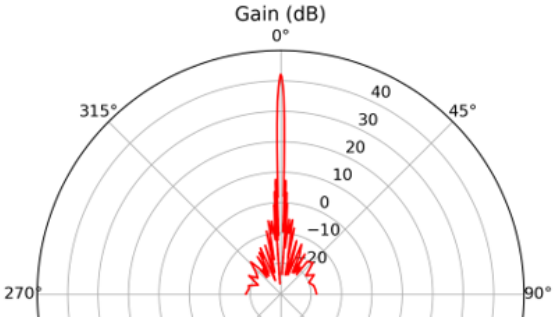

Figure A.1: *Simulated radiation profile of the EST X-band antenna. The antenna has a Half Power Beam Width (HPBW) of around 1.1°.*

A.2 Free space path loss

Evolution of the free space path loss (FSPL) computed with Eq.2.3 from the results of a satellite simulation made with `satastro`. Fig.A.2 shows how the FSPL changes as the satellite moves between the horizon (0° of elevation) and the zenith (90° of elevation). By considering that the minimal communication elevation is 10°, the FSPL varies of 10 dB in the case of a satellite passing exactly over the ground station. This simulation has been made for a satellite on a LEO orbit, at an altitude of 557km [5].

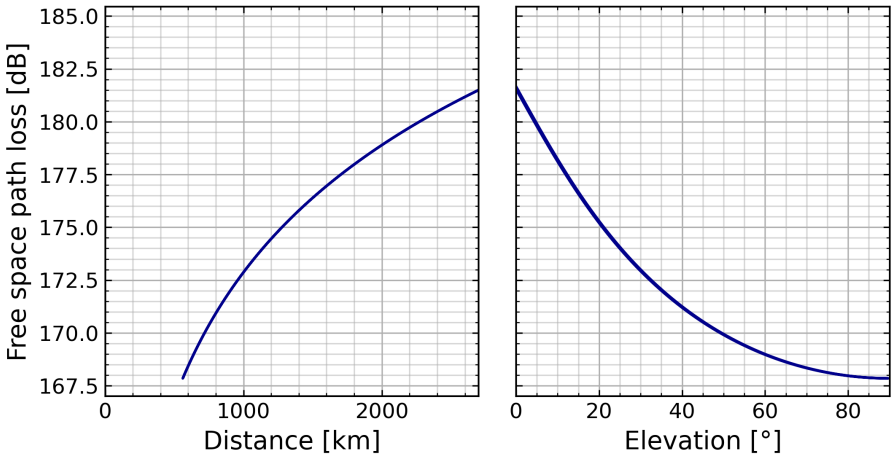

Figure A.2: *Evolution of the free space path loss as a function of the distance and elevation of a satellite in a 557km high orbit, viewed from a ground station.*

B Spiral search algorithm

The following Python code generates the spiral points used for spiral search in 3.2. It is an Archimedean spiral defined by three parameters: the total radius of the spiral `radius`, the distance between two arms of the spiral `r_spacing` and the distance between two points of the spiral `points_spacing`. The spiral has additional points in the centre to cover it better. The result can be observed in Fig.3.5.

```
def spiral_points(radius, r_spacing, points_spacing):
    """
    Generate spiral points

    Parameters
    ----------
    radius : float
        Max radius of spiral
    r_spacing : float
        Radial spacing
    points_spacing : float
        Points spacing

    Returns
    -------
    points : np.array
        The spiral points
    """
    points = [(0,0)]
    angle = points_spacing/r_spacing*2*np.pi
    r = r_spacing*angle/(2*np.pi)
    # Better sampling around center
    for i in np.arange(np.pi/3+angle,2*np.pi+angle,np.pi/3):
        x = points_spacing*np.cos(i)*np.sqrt((i-angle)/(2*np.pi))
        y = points_spacing*np.sin(i)*np.sqrt((i-angle)/(2*np.pi))
        points.append([x, y])
    # Archimedes spiral
    while r < radius:
        r = r_spacing*angle/(2*np.pi)
        x = r*np.cos(angle)
        y = r*np.sin(angle)
        points.append([x, y])
        angle += points_spacing/r
    return np.array(points)
```

References

[1] Dorian Agrati. *Conception of an autonomous calibration system for a X-Y antenna pointing mechanism*. Tech. rep. EPFL Spacecraft Team, 2024.

[2] Saika Aida and Michael Kirschner. "Accuracy Assessment of SGP4 Orbit Information Conversion into Osculating Elements". In: *6th European Conference on Space Debris*. Ed. by ESA/ESOC. 2013. URL: https://conference.sdo.esoc.esa.int/proceedings/sdc6/paper/41/SDC6-paper41.pdf.

[3] Astropy Collaboration et al. "The Astropy Project: Sustaining and Growing a Community-oriented Open-source Project and the Latest Major Release (v5.0) of the Core Package". In: *The Astrophysical Journal* 935.2, 167 (Aug. 2022), p. 167. DOI: 10.3847/1538-4357/ac7c74. arXiv: 2206.14220 [astro-ph.IM].

[4] Michaël Baudin et al. "OpenTURNS: An Industrial Software for Uncertainty Quantification in Simulation". In: *Handbook of Uncertainty Quantification*. Ed. by Roger Ghanem, David Higdon, and Houman Owhadi. Cham: Springer International Publishing, 2016, pp. 1–38. ISBN: 978-3-319-11259-6. DOI: 10.1007/978-3-319-11259-6_64-1. URL: https://doi.org/10.1007/978-3-319-11259-6_64-1.

[5] Adrien Dupont and Léonard Lebrun. *Chess Pathfinder 1 Mission - Link Budget: X-band*. Tech. rep. EPFL Spacecraft Team, 2024.

[6] T. Flohrer, H. Krag, and H. Klinkrad. "Assessment and Categorization of TLE Orbit Errors for the US SSN Catalogue". In: *Advanced Maui Optical and Space Surveillance Technologies Conference*. Ed. by C. Paxson et al. Jan. 2008, E53, E53.

[7] Donald Jones, Matthias Schonlau, and William Welch. "Efficient Global Optimization of Expensive Black-Box Functions". In: *Journal of Global Optimization* 13 (Dec. 1998), pp. 455–492. DOI: 10.1023/A:1008306431147.

[8] Léonard Lebrun. *Antenna Design in S/X band for a 2.4m parabolic reflector*. Tech. rep. EPFL Spacecraft Team, 2023.

[9] pericynthion. *What is the accuracy / uncertainty of Two Line Elements (TLEs)?* Space.StackEchange.com. 2014.

[10] Juan Luis Cano Rodríguez et al. *poliastro/poliastro: poliastro 0.17.0 (SciPy US '22 edition)*. Version v0.17.0. July 2022. DOI: 10.5281/zenodo.6817189. URL: https://doi.org/10.5281/zenodo.6817189.

[11] Valentin Suppa-Gallezot. *Design of a new X-Y satellite tracking mount for X-band communication*. Tech. rep. EPFL Spacecraft Team, 2023.